



Contents lists available at ScienceDirect

Spectrochimica Acta Part A: Molecular and Biomolecular Spectroscopy

journal homepage: www.elsevier.com/locate/saa

Synthesis, characterization and quantum chemical investigation of molecular structure and vibrational spectra of 2,5-dichloro-3,6-bis-(methylamino)1,4-benzoquinone

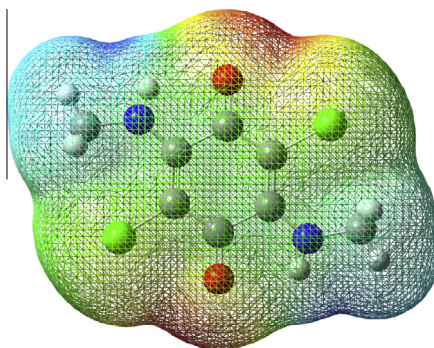
Bhanu Pratap Singh Gautam^a, Mayuri Srivastava^b, R.L. Prasad^{a,*}, R.A. Yadav^{b,*}^a Department of Chemistry, Banaras Hindu University, Varanasi 221005, India^b Department of Physics, Banaras Hindu University, Varanasi 221005, India

HIGHLIGHTS

- 2,5-Dichloro-3,6-bis-(methylamino)1,4-benzoquinone (dmdb) has been synthesized and characterized.
- FT-IR spectra and FT-Raman of dmdb have been recorded and analyzed.
- Molecular structure, NBO analysis, HOMO–LUMO analysis, MESP and thermodynamic functions have been computed and analyzed.

GRAPHICAL ABSTRACT

MEP plot of dmdb molecule is reproduced here.



ARTICLE INFO

Article history:

Received 18 October 2013

Received in revised form 11 February 2014

Accepted 19 February 2014

Available online 22 March 2014

Keywords:

Quinones
DFT calculation
Ab initio calculations
Optimized geometry
NBO analysis
MESP

ABSTRACT

2,5-Dichloro-3,6-bis-methylamino-[1,4]benzoquinone has been synthesized by condensing methyl amine hydrochloride with chloranil in presence of condensing agent sodium acetate. FT-IR (4000–400 cm^{-1}) and FT-Raman (4000–400 cm^{-1}) spectral measurements of dmdb have been done. *Ab initio* and DFT (B3LYP/6-311+G**) calculations have been performed giving energies, optimized structures, harmonic vibrational frequencies, infrared intensities and Raman activities. The optimized molecular structure of the compound is found to possess C_{2h} point group symmetry. A detailed interpretation of the observed IR and Raman spectra of dmdb is reported on the basis of the calculated potential energy distribution. Stability of the molecule arising from hyper conjugative interactions, charge delocalization has been analyzed using NBO analysis. The HOMO and LUMO energy gap reveals that the energy gap reflects the chemical activity of the molecule. The thermodynamic functions of the title compound have also been computed.

© 2014 Elsevier B.V. All rights reserved.

Introduction

Quinones form a large group of compounds with various biological activities. These are found in many animal and plant cells

and are extensively used as anticancer, antibacterial or antimalarial drugs as well as fungicides [1,2]. Quinones are involved in various bioenergetic processes as important transport agents. These compounds have also attracted considerable attention because of their biological activities and chemotherapeutic values. Various quinones containing oxygenated aromatic rings have been reported to possess biological activities [3–5]. A group of 1,4-benzoquinones

* Corresponding authors. Tel.: +91 5422368593 (R.A. Yadav).

E-mail addresses: rayadav@bhu.ac.in, ray1357@gmail.com (R.A. Yadav).

and their nitrogen analogues have been reported for their antitumor activities [6–8]. Quinones that act against animal tumours are believed to function as bio-reductive alkylating agents [9–11] and play important roles in biological functions including a role in oxidative phosphorylation and electron transfer [12,13]. Besides, they have found many technical applications and also represent important synthetic building blocks. Quinones [14–17] and the parent p-quinols [18] are found as structural units in a variety of bioactive natural compounds showing antigerminative, antifungal, antibacterial, antiviral and anticancer activities. Hence, they are useful intermediates for organic synthesis with particular interest into the production of biologically active compounds [19–22], e.g. trimethyl-1,4-benzoquinone is a key reagent in the synthesis of vitamin E and 2-methyl-1,4-naphthoquinone (vitamin K₃), an important additive in animal feed, is also utilized for construction of vitamin K₁ [23]. From the point of view of electron transfer reactions, benzoquinones play an important role in biological systems [12,24–26]. 1,4-Benzoquinone is one of the most important and fundamental p-electron systems because of its high electron affinity and photoreactivity [27,28]. Molecules with the quinoid structure form one of the most attractive classes of compounds in organic chemistry. The chemistry of quinones is largely dependent on the substituents being either on the quinonic or on adjacent rings. This is reflected in their chemical reactivity, especially in heterocyclic quinones [29]. DFT method is shown to predict accurately molecular properties such as optimized structure, vibrational frequencies, energy, charge distributions on atoms of a molecule and point group symmetry.

In the present paper we have synthesized and characterized 2,5-dichloro-3,6-bis-methylamino-[1,4]benzoquinone (abbreviated as dmdb) which consists of π -conjugated double bonds and is capable of forming molecular complexes like chloranilic acid. Further, since dmdb molecule possesses alternate double bonds, it is expected to be a good candidate for molecular conductors. In this paper we present the results of the IR and Raman spectral study and vibrational analysis in light of the DFT calculations at the B3LYP/6-311++G** level using the Gaussian 09 package for supporting experimental results and vibrational assignments. In addition molecular structure, charges on atomic sites, Natural Bond Orbital (NBO) analysis, HOMO–LUMO analysis, molecular electrostatic potential (MESP) and thermodynamic functions have been computed and analyzed for dmdb (lowest energy conformer C-1).

Experimental

Material and instrumentation

All the chemicals used under the present investigation were of analytical reagent (A R) grade. 2,3,5,6-Tetrachloro-1,4-benzoquinone was purchased from the Merck and used as such without further purification. The elemental analysis was done on a Perkin–Elmer CHN analyzer model-240C. ¹H NMR spectra were recorded on a JEOL AL 300 MHz multinuclear NMR spectrometer using *d*₆-DMSO as solvent and TMS as an internal reference. The IR spectrum of the solid sample was recorded on a JASCO FTIR spectrometer model-5300 in KBr pellet in the spectral range 4000–400 cm⁻¹. Following experimental parameters were used for recording the IR spectra: resolution – 4 cm⁻¹; gain-20; scan-100. The Raman spectrum of the molecule has been recorded in the region 4000–400 cm⁻¹, on a Jobin Yvon HORIBA HR 800 Raman spectrometer using 488 nm line of an Ar⁺ laser for excitation with the following parameters: laser spot size: 1 cm⁻¹, resolution ~1 cm⁻¹, power at the sample <10 mW, integration time: 10 s, one window covers ~800 cm⁻¹, accuracy of measurements – 2 cm⁻¹, slit-width fixed at the entrance of laser 200 μ m.

Synthesis of 2,5-dichloro-3,6-bis-methylamino-[1,4]benzoquinone

For the synthesis of 2,5-dichloro-3,6-bis-methylamino-[1,4]benzoquinone (dmdb), sodium acetate (1.148 g, 14 mmol) was added pinch by pinch in 20 min to a reaction mixture of chloranil (0.492 g, 2 mmol) added dropwise methylamine hydrochloride (0.270 g, 4 mmol) in 15 ml absolute ethanol with constant stirring for 15 min at room temperature. The color of the reaction mixture slowly changed from yellow to dark brown. The stirring was continued for 1 h and refluxed for 4 h. The resulting dark brown precipitated product was filtered off, washed three times with water, ethanol–water mixture followed by ethanol and dried under vacuo over calcium chloride.

Computational details

To optimize the structure of 2,5-dichloro-3,6-bis-methylamino-1,4-benzoquinone, the following procedure was adopted, initially the structure of p-diamino benzene was optimized. In the optimized structure of p-diamino benzene one methyl group is attached at N₁₁ position. Out of the two possible conformers one with the lower energy was taken and another methyl group at the position N₁₃ was added. Now by taking different orientations of the –CH₃ group geometries were optimized. With the minimum energy conformer one oxygen atom is attached at the position C₅ and another at the position C₂ and the structure was again optimized. To this minimum energy conformer one chlorine atom is attached at the position C₁ and C₄ and the structure was further optimized at the B3LYP/6-311++G** level. The geometry was fully optimized without any constraint. Since there is C₄ axis therefore 2⁴ = 16 conformers are possible. But because of symmetry regions the total numbers of conformers are 10 only and the lowest energy conformer is considered.

The optimized molecular geometries, APT charges, natural charges and fundamental vibrational wave numbers along with their corresponding intensities in IR spectrum, Raman activities and depolarization ratios of the Raman bands for the lowest energy conformer of dmdb molecule were computed by using Gaussian 09 package program [30] with molecular visualization program [31] on the personal computer at B3LYP method at 6-311++G(d,p) [32–36] calculation level. In order to obtain the reasonable frequency matching, scale factors proposed by Rauhut and Pulay [37] were employed. The assignments of all the normal modes of vibration have been made on the basis of the calculated potential energy distributions (PEDs). For the calculation of the PEDs the vibrational problem was set up in terms of internal coordinates using gar2ped software. The observed IR and Raman frequencies corresponding to the fundamental modes have been correlated to the calculated fundamental frequencies in light of the PEDs. The molecular electrostatic potential (MESP) surface, which is used for predicting sites and relative reactivity towards electrophilic attack and in studies of biological recognition and hydrogen bonding interactions, has been plotted and the NBO analysis has been carried out in order to investigate intra-molecular charge-transfer (CT) interactions, rehybridisation and delocalization of electron density (ED) within the molecule.

Results and discussions

Characterization of the 2,5-dichloro-3,6-bis-methylamino-[1,4]benzoquinone

Physical methods

The compound is insoluble in common organic solvents like ethanol, chloroform and dichloromethane, etc. but on heating it

is slight soluble in Acetone, Acetonitrile and also soluble in polar solvents like DMF and DMSO. It is dark brown powder, Yield 85% and mp is >290 °C.

Chemical methods

The synthesized dmdb molecule has been successfully characterized by elemental analysis, ^1H NMR and ^{13}C NMR. The C, H, N analysis of the compound is well within the range of calculated values as: Anal. Calc. for $\text{C}_8\text{H}_8\text{N}_2\text{O}_2\text{Cl}_2$: C, 40.86%; H, 3.42%; N, 11.91%. Found: C, 40.65%; H, 3.35%; N, 11.94%. ^1H NMR spectrum of dmdb (Fig. 1) exhibits $-\text{CH}_3$ proton at 3.11 δ and $>\text{N}-\text{H}$ proton at 7.77 δ and the ^{13}C NMR spectrum of dmdb (Fig. 2) molecule in d_6 -DMSO shows four signals at 172.65, 151.60, 101.11 and 31.8 δ . The signal at 172.65 δ corresponds to the carbon atoms (C_2 and C_5) attached to the quinone moiety, that at 151.60 δ corresponds to the carbon atoms (C_1 and C_4) attached to the chlorine atoms, the signal at 101.11 δ corresponds to the carbon atoms (C_3 and C_6) attached to the methylamino group and the signal at 31.81 δ corresponds to the methyl carbon atoms.

Molecular geometry

The optimized geometrical structure and the atomic labeling scheme corresponding to the conformer (C-I) are shown in Fig. 3 and optimized geometrical structures, their total energies and relative energies (in different units) of all the 10 possible conformers of dmdb are shown in Table 1. The optimized geometrical parameters of the dmdb (C-I) are collected in Table 2. The geometrical structure shows that all the atoms lie in a plane and the optimized molecular structure possesses C_{2h} point group symmetry. The C_3 and C_6 are attached with methyl amino group; the C_1 and C_4 are attached with an oxygen atom. The four hydrogen atoms namely H_{17} , H_{19} , H_{21} and H_{22} are symmetrically up and down the benzene ring whereas H_{18} and H_{20} are in the plane of the benzene ring.

Optimized structure of the dmdb molecule shows that the ring bonds C_1-C_2 and C_4-C_5 have partial double bond character; the ring bonds C_2-C_3 and C_5-C_6 have single bond character and the ring bonds C_3-C_4 and C_1-C_6 have double bond character. The present structural data could be compared with those of 2,5-diamino-3,6-dichloro-1,4-benzoquinone (dadb) [38]. The magnitude of the bond length C_3-N_{11} and C_6-N_{13} is similar to the case of dadb molecule. Bond lengths C_3-N_{11} and C_6-N_{13} indicate that both C_3-N_{11} and C_6-N_{13} possess double bond character. No major changes are

found in the bond lengths C–C, C–H, N–H, C–Cl and C–O from their corresponding usual bond lengths. The internal bond angles $\alpha(\text{C}_1-\text{C}_2-\text{C}_3)$, $\alpha(\text{C}_2-\text{C}_3-\text{C}_4)$, $\alpha(\text{C}_3-\text{C}_4-\text{C}_5)$, $\alpha(\text{C}_4-\text{C}_5-\text{C}_6)$, and $\alpha(\text{C}_5-\text{C}_6-\text{C}_1)$ of the benzene ring are found to be 119°, 120°, 122°, 119° and 120° respectively in dmdb in good agreement with the respective experimental values 117°, 122°, 122°, 117° and 122° in the dadb molecule. All the dihedral angles corresponding to the atoms H_{12} , H_{14} , H_{21} and H_{17} of benzene ring are either 0° or $\pm 180^\circ$. The dihedral angle $\delta(\text{C}_1-\text{C}_6-\text{N}_{13}-\text{C}_{15})$ is greater than $\delta(\text{C}_4-\text{C}_3-\text{N}_{11}-\text{C}_{16})$ by $\sim 15^\circ$.

Atomic charges

APT charges at various atoms of dmdb molecule (C-I) calculated at the B3LYP/6-311++G** level are collected in Table 3. The six carbon atoms of dmdb form three pairs with nearly equal charges at (C_1 , C_4), (C_2 , C_5) and (C_3 , C_6). It is note worthy to mention that C_1 and C_4 atoms of dmdb exhibit negative charges where as C_2 , C_3 , C_5 and C_6 atoms exhibit positive charges and magnitude of charges on C_2 and C_5 are more than those on C_3 and C_6 . The magnitude of charges calculated on both O atoms is equal and negative. Its value is found to be 0.84 a.u. corresponding to the atoms O_7 and O_8 respectively. The magnitudes of charges calculated on both N atoms are also negative with equal magnitudes 0.77 a.u. respectively. Similar trend is being observed for the charges on Cl atoms. Due to high electronegativity all the O, Cl and N atoms possess negative APT charges. The four hydrogen atoms H_{17} , H_{19} , H_{21} and H_{22} possess negative and equal charges with magnitude 0.01 a.u. The charges on H_{18} and H_{20} atoms, coplanar with the benzene ring, are positive and equal with magnitudes 0.00 a.u. The remaining two hydrogen atoms, facing towards oxygen atoms, H_{12} and H_{14} exhibit more positive and equal charges with magnitudes 0.28 a.u. Thus, higher charges on H_{12} and H_{14} atoms as compared to those on H_{18} and H_{20} arise as a consequence of involvement of former pair of atoms in hydrogen bonding with oxygen atoms (Table 3). Mulliken atomic charges on different atomic sites of dmdb molecule (C-I) and its ions are collected in supplementary material (Table 1).

Vibrational assignments

2,5-Dichloro-3,6-bis-methylamino-1,4-(benzoquinone) is a non-planar molecule having molecular symmetry C_{2h} . Since dmdb

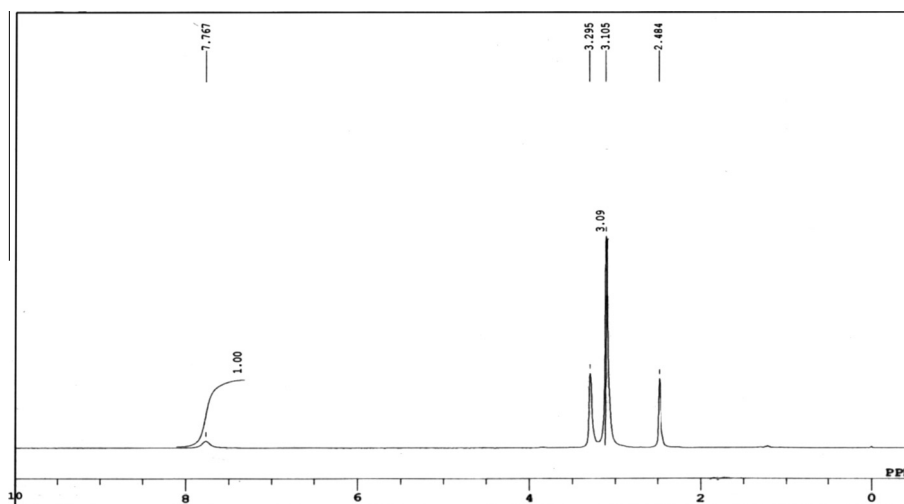


Fig. 1. ^1H NMR spectra of 2,5-dichloro-3,6-bis-methylamino-[1,4]benzoquinone.

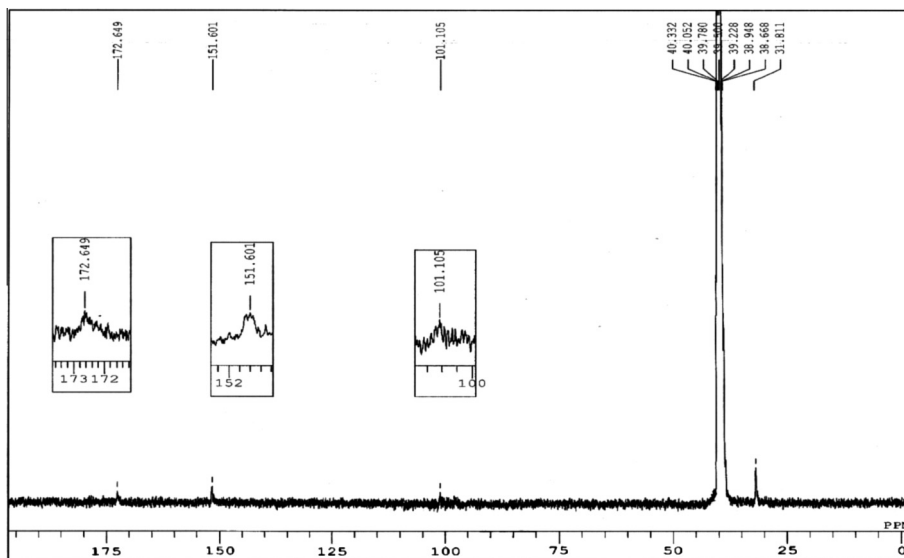


Fig. 2. ^{13}C NMR spectra of 2,5-dichloro-3,6-bis-methylamino-[1,4]benzoquinone.

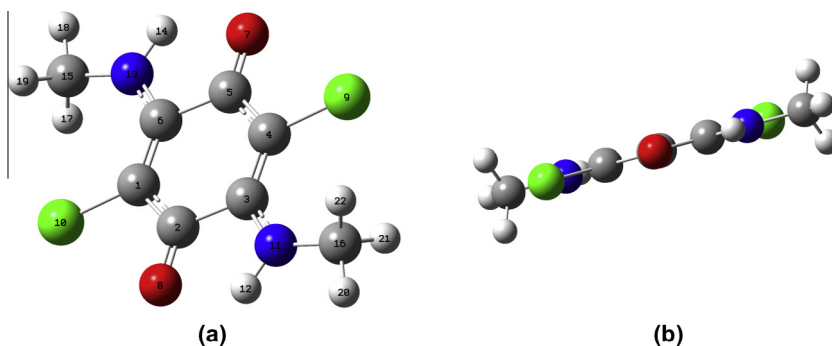


Fig. 3. Optimized molecular structure and leveling scheme of (a) front view and (b) side view of 2,5-dichloro-3,6-bis-methylamino-[1,4]benzoquinone (dmdb).

contains 22 atoms it possesses 60 normal modes of vibrations which are distributed among its four symmetry species as $20A_g + 11A_u + 10B_g + 19B_u$. Because of inversion symmetry the A_g and B_g modes are Raman active and IR forbidden while A_u and B_u modes are IR active and Raman forbidden i.e. principal of mutual exclusion is applicable for the dmdb molecule. The observed and calculated IR and Raman spectra of PTA are reproduced in Figs. 4 and 5 respectively.

The normal modes distribution could be divided under the following sections: (i) CH_3 group modes (18 modes), (ii) Ring modes (12 modes), (iii) C—Cl modes (6 modes), (iv) C=O modes (6 modes), (v) N— CH_3 modes (6 modes), (vi) C—NH (CH_3) modes (6 modes) and (vii) N—H modes (6-modes). The distributions of normal modes of vibration of dmdb molecule are shown in Table 4 and the calculated and observed vibrational frequencies with the corresponding PEDs and assignments for dmdb molecule (C-I) are collected in Table 5.

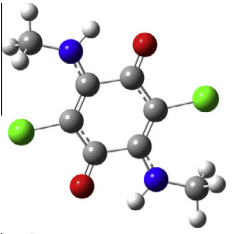
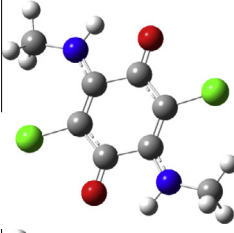
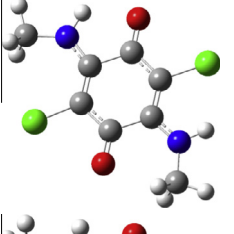
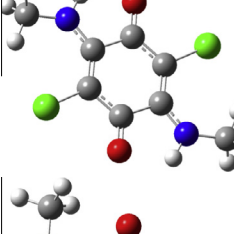
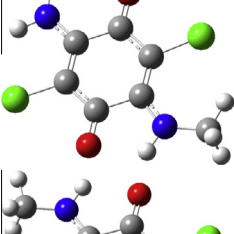
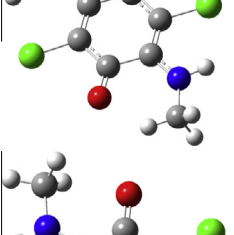
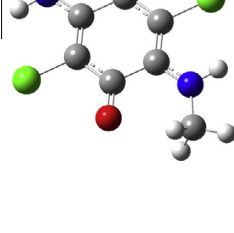
CH_3 group modes (18 modes)

There are 9 normal modes due to a CH_3 group, namely, two anti-symmetric CH_3 stretching (ν_{as}), a symmetric CH_3 stretching (ν_s), a parallel rocking mode (ρ_{\parallel}), a perpendicular rocking mode (ρ_{\perp}), a twisting mode (τ), two asymmetric deformations (δ_{as}) and one symmetric deformation (δ_s). Thus the two CH_3 groups have 18 normal modes of vibrations. Due to nearly equal magnitudes the

normal modes of vibrations of one CH_3 group are expected to couple strongly with the corresponding modes of the other CH_3 group. As the molecule dmdb belongs to the C_{2h} point group, one of the coupled modes (in phase coupled (i.p. coupled)) of planar vibration is expected to belong to the A_g species while the other coupled mode (out-of-phase coupled (o.p. coupled)) belong to the B_u species. Similarly, one of the coupled modes (o.p. coupled) due to non-planar vibrations belongs to the A_u species and other coupled mode (i.p. coupled) belongs to the B_g species.

The present calculations give rise to four ν_{as} modes in which two ν_{as} modes having equal magnitude (2990 cm^{-1}) and another two ν_{as} modes having equal magnitude (2978 cm^{-1}). Similarly the two coupled ν_s modes are also expected and observed at equal frequency 2915 cm^{-1} . The two coupled parallel rocking modes of the CH_3 group are found at frequencies 1129 cm^{-1} (i.p.c.) and 1138 cm^{-1} (o.p.c.). Similarly the two coupled perpendicular rocking modes of the CH_3 groups correspond to equal frequency 1087 cm^{-1} . The two asymmetric deformation modes of the CH_3 groups are found at equal frequency 1440 cm^{-1} and the rest of two δ_{as} have equal magnitude 1423 cm^{-1} . Magnitude 1397 cm^{-1} (o.p.c.) and 1400 cm^{-1} (i.p.c.) refer coupled symmetric deformation modes of the two CH_3 groups. Out of the two coupled CH_3 twisting modes $\tau(\text{CH}_3)$, one corresponding to the A_u Species is calculated to have magnitude 169 cm^{-1} and rest one corresponding to the B_g species has frequency 172 cm^{-1} .

Table 1
Optimized structures, total energies and relative energies of all the 10 possible conformers of dmdb.

S. no.	Optimized structure	Conformers	Total energy (Hartree)	Relative energy		
				Hartree	Temp. (K)	kcal/mol
1		C-I	-1490.21074183	0	0	0
2		C-II	-1490.20887423	0.00186760	640	1.26
3		C-III	-1490.20803159	0.00271024	960	1.89
4		C-IV	-1490.20698788	0.00375395	1280	2.52
5		C-V	-1490.20609893	0.00464290	1600	3.15
6		C-VI	-1490.20544374	0.00529809	1600	3.15
7		C-VII	-1490.20541854	0.00532329	1600	3.15

(continued on next page)

Table 1 (continued)

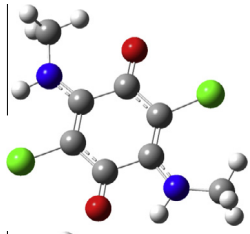
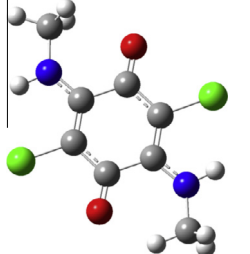
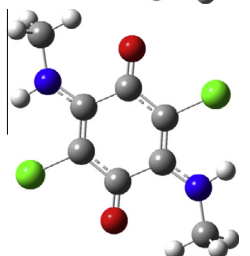
S. no.	Optimized structure	Conformers	Total energy (Hartree)	Relative energy		
				Hartree	Temp. (K)	kcal/mol
8		C-VIII	-1490.20351273	0.00722910	2240	4.41
9		C-IX	-1490.20297594	0.00776589	2560	5.04
10		C-X	-1490.20051814	0.01022369	3200	6.30

Table 2 Geometrical parameters^a of dmdb molecule (C-I).

Parameters	dmdb molecule			dad ^b molecule	Difference dmdb (neutral)-dad ^b (neutral)
	Neutral	Cation (+)	Anion (-)		
C ₁ -C ₂	1.435	1.456	1.429	1.437	-0.002
C ₂ -C ₃	1.545	1.527	1.485	1.531	0.014
C ₃ -C ₄	1.373	1.401	1.385	1.367	0.006
C ₄ -C ₅	1.435	1.456	1.429	1.437	-0.002
C ₅ -C ₆	1.545	1.527	1.485	1.531	0.014
C ₆ -C ₁	1.373	1.401	1.385	1.437	-0.064
C ₁ -Cl ₁₀	1.758	1.711	1.783	1.749	0.009
C ₄ -Cl ₉	1.758	1.711	1.783	1.749	0.009
C ₂ -O ₈	1.225	1.215	1.263	1.222	0.003
C ₅ -O ₇	1.225	1.215	1.263	1.222	0.003
C ₃ -N ₁₁	1.335	1.318	1.371	1.336	-0.001
C ₆ -N ₁₃	1.335	1.318	1.371	1.336	-0.001
N ₁₁ -H ₁₂	1.018	1.023	1.016	-	-
N ₁₁ -H ₁₃	-	-	-	1.007	-
N ₁₁ -H ₁₄	-	-	-	1.012	-
N ₁₃ -H ₁₄	1.018	1.023	1.016	-	-
N ₁₂ -N ₁₅	-	-	-	1.012	-
N ₁₂ -N ₁₆	-	-	-	1.007	-
N ₁₁ -C ₁₆	1.458	1.466	1.443	-	-
N ₁₃ -C ₁₅	1.458	1.466	1.443	-	-
C ₁₅ -H ₁₇	1.090	1.089	1.095	-	-
C ₁₅ -H ₁₈	1.089	1.088	1.094	-	-
C ₁₅ -H ₁₉	1.090	1.089	1.095	-	-
C ₁₆ -H ₂₀	1.089	1.088	1.094	-	-
C ₁₆ -H ₂₁	1.090	1.089	1.095	-	-
C ₁₆ -H ₂₂	1.090	1.089	1.095	-	-
O ₇ ···N ₁₁	-	-	-	2.625	-
O ₈ ···H ₁₂	1.968	1.990	1.969	-	-
O ₇ ···H ₁₄	-	-	-	2.182	-
O ₇ ···H ₁₇	4.568	4.573	4.587	-	-
O ₇ ···H ₁₈	4.229	4.242	4.243	-	-

Table 2 (continued)

Parameters	dmdb molecule			dadb ^b molecule		Difference dmdb (neutral)–dadb (neutral)
	Neutral	Cation (+)	Anion (–)	Neutral		
O ₇ ··H ₁₉	4.569	4.574	4.591	–	–	–
O ₈ ··H ₂₀	4.229	4.242	4.232	–	–	–
O ₈ ··H ₂₁	4.569	4.574	4.591	–	–	–
O ₈ ··H ₂₂	4.568	4.573	4.587	–	–	–
O ₈ ··N ₁₂	–	–	–	1.625	–	–
O ₇ ··H ₁₄	1.968	1.990	1.969	–	–	–
O ₈ ··H ₁₅	–	–	–	2.182	–	–
Cl ₉ ··N ₁₁	–	–	–	3.056	–	–
Cl ₉ ··H ₁₂	4.244	4.219	4.241	2.680	–	1.564
Cl ₉ ··H ₂₀	4.239	4.229	4.228	–	–	–
Cl ₉ ··H ₂₁	2.921	2.914	2.908	–	–	–
Cl ₉ ··H ₂₂	2.921	2.913	2.911	–	–	–
Cl ₁₀ ··N ₁₂	–	–	–	3.056	–	–
Cl ₁₀ ··H ₁₄	4.244	4.219	4.241	–	–	–
Cl ₁₀ ··H ₁₆	–	–	–	2.680	–	–
Cl ₁₀ ··H ₁₇	2.921	2.913	2.911	–	–	–
Cl ₁₀ ··H ₁₈	4.239	4.229	4.228	–	–	–
Cl ₁₀ ··H ₁₉	2.921	2.914	2.908	–	–	–
C ₁ –C ₂ –C ₃	118.8	119.1	116.9	116.8	–	2
C ₂ –C ₃ –C ₄	119.6	119.5	119.4	121.4	–	–1.8
C ₃ –C ₄ –C ₅	121.6	121.4	123.6	121.8	–	–0.2
C ₄ –C ₅ –C ₆	118.8	119.1	116.9	116.8	–	2
C ₅ –C ₆ –C ₁	119.6	119.5	119.4	121.4	–	1.8
C ₆ –C ₁ –C ₂	121.6	121.4	123.6	121.8	–	–0.2
C ₃ –C ₂ –O ₈	116.9	117.6	118.4	117.6	–	–0.7
C ₁ –C ₂ –O ₈	124.2	123.2	124.6	125.5	–	–1.3
C ₄ –C ₅ –O ₇	124.2	123.2	124.6	125.5	–	–1.3
C ₆ –C ₅ –O ₇	116.9	117.6	118.4	117.6	–	–0.7
C ₃ –C ₄ –Cl ₉	123.5	123.6	122.0	120.3	–	3.2
C ₅ –C ₄ –Cl ₉	114.9	115.1	114.4	118.0	–	–3.1
C ₂ –C ₁ –Cl ₁₀	114.9	115.1	114.4	118.0	–	–3.1
C ₆ –C ₁ –Cl ₁₀	123.5	123.6	122.0	120.3	–	3.2
C ₂ –C ₃ –N ₁₁	109.9	111.0	110.6	113.0	–	–3.1
C ₄ –C ₃ –N ₁₁	130.5	129.5	129.9	125.6	–	4.9
C ₅ –C ₆ –N ₁₃	109.9	111.0	110.6	113.0	–	–3.1
C ₁ –C ₆ –N ₁₃	130.5	129.5	129.9	125.6	–	4.9
C ₃ –N ₁₁ –H ₁₂	110.9	111.1	109.4	121.4	–	–10.5
C ₂ –N ₁₁ –H ₁₄	–	–	–	117.3	–	–
C ₃ –N ₁₁ –C ₁₆	131.1	132.1	131.2	–	–	–
C ₆ –N ₁₃ –H ₁₄	110.9	111.1	109.4	–	–	–
C ₅ –N ₁₂ –H ₁₅	–	–	–	117.3	–	–
C ₆ –N ₁₃ –C ₁₅	131.1	132.1	131.2	121.4	–	9.7
H ₁₃ –N ₁₁ –H ₁₄	–	–	–	–	–	–
H ₁₄ –N ₁₃ –C ₁₅	117.9	116.9	119.4	–	–	–
H ₁₆ –N ₁₃ –H ₁₅	–	–	–	–	–	–
N ₁₃ –C ₁₅ –H ₁₇	111.7	110.8	112.8	–	–	–
N ₁₃ –C ₁₅ –H ₁₈	107.2	107.1	107.4	–	–	–
N ₁₃ –C ₁₅ –H ₁₉	111.7	110.8	112.8	–	–	–
H ₁₇ –C ₁₅ –H ₁₈	108.7	109.3	108.0	–	–	–
H ₁₈ –C ₁₅ –H ₁₉	108.7	109.3	108.0	–	–	–
H ₁₇ –C ₁₅ –H ₁₉	108.8	109.5	107.5	–	–	–
N ₁₁ –C ₁₆ –H ₂₀	107.2	107.1	107.4	–	–	–
N ₁₁ –C ₁₆ –H ₂₁	111.7	110.8	112.8	–	–	–
N ₁₁ –C ₁₆ –H ₂₂	111.7	110.8	112.8	–	–	–
H ₂₀ –C ₁₆ –H ₂₁	108.7	109.3	108.0	–	–	–
H ₂₀ –C ₁₆ –H ₂₂	108.7	109.3	108.0	–	–	–
H ₂₁ –C ₁₆ –H ₂₂	108.8	109.5	107.5	–	–	–

^a Bond lengths in Å and angles in degrees.

^b From Ref. [38].

Quinoid ring modes

In the present case the quinoid ring contain two C=C bonds and four C–C bonds, therefore, one expects two ring stretching modes corresponding to the C=C stretching motions and four ring stretching modes corresponding to the four C–C stretching motions.

The i.p. coupled and o.p. coupled C=C stretching modes are calculated to have equal magnitude 2915 cm^{–1} out of the remaining four stretching modes, the two higher modes are calculated to be at 1280 cm^{–1} (A_g species) and 1277 cm^{–1} (B_u species). The fifth ring stretching mode is calculated to be at 957 cm^{–1} corresponding

to the species B_u and the sixth ring stretching mode corresponding to the A_g species and is calculated to have a magnitude of 541 cm^{–1}. The three planar ring deformation modes of the quinoid ring are calculated to have magnitude 274, 340 and 588 cm^{–1} and the three non-planar ring deformation modes correspond to frequencies 64, 577 and 741 cm^{–1}.

C–Cl modes (6 modes)

In benzene derivatives [39] C–Cl stretching is observed in wide spectral range 700–1050 cm^{–1}. The present calculations place the

Table 3
Calculated APT Charges^a of dmb molecule (C-I).

Atom	dmb molecule			Dadb ^b molecule
	Neutral	Cation (+)	Anion (-)	Neutral
C ₁	-0.27	0.67	0.54	0.98
C ₂	0.99	0.18	0.55	0.48
C ₃	0.55	0.45	0.54	-0.20
C ₄	-0.27	0.67	0.52	0.98
C ₅	0.99	0.18	0.55	0.48
C ₆	0.55	0.45	0.54	-0.20
O ₇	-0.84	-0.48	-0.91	-0.80
O ₈	-0.84	-0.48	-0.91	-0.80
Cl ₉	-0.28	-0.34	-0.38	-0.28
Cl ₁₀	-0.28	-0.34	-0.38	-0.28
N ₁₁	-0.77	-0.49	-0.89	-0.73
N ₁₃	-0.77	-0.49	-0.89	-0.73
H ₁₂	0.28	0.15	0.23	0.25
H ₁₄	0.28	0.15	0.23	0.31
C ₁₅	0.37	0.28	0.50	-
C ₁₆	0.37	0.28	0.50	-
H ₁₇	-0.01	0.01	-0.07	-
H ₁₈	0.00	0.05	-0.05	-
H ₁₉	-0.01	0.01	-0.07	-
H ₂₀	0.00	0.05	-0.05	-
H ₂₁	-0.01	0.01	-0.07	-
H ₂₂	-0.01	0.01	-0.07	-

^a In unit of e.^b From Ref. [38].

i.p. coupled C–Cl stretching mode (A_g species) at frequency 860 cm^{-1} and o.p. coupled C–Cl stretching mode (B_u species) at 757 cm^{-1} . The modes corresponding to the i.p. coupled planar deformation mode (A_g species) and o.p. coupled planar deformation mode (B_u species) are at frequencies 217 and 225 cm^{-1} respectively. The magnitudes 275 and 194 cm^{-1} correspond to the modes $\gamma(\text{C–Cl})$ i.p. coupled and $\gamma(\text{C–Cl})$ o.p. coupled respectively.

C=O modes (6 modes)

The two (C=O) bonds give rise to six normal modes of vibration as $2\nu(\text{C=O})$, $2\beta(\text{C=O})$ and $2\gamma(\text{C=O})$ modes. The C=O stretching frequency appear strongly in the range $1600\text{--}1850\text{ cm}^{-1}$. The frequencies 1617 and 1638 cm^{-1} corresponding to the C=O stretching modes. The present calculations also place the i.p. coupled $\beta(\text{C=O})$ at 773 cm^{-1} (A_g species) and o.p. coupled $\beta(\text{C=O})$ at

414 cm^{-1} (B_u species) and similarly i.p. coupled $\gamma(\text{C=O})$ (B_g species) at 524 cm^{-1} and o.p. coupled $\gamma(\text{C=O})$ (A_u species) at 748 cm^{-1} .

N–CH₃ modes

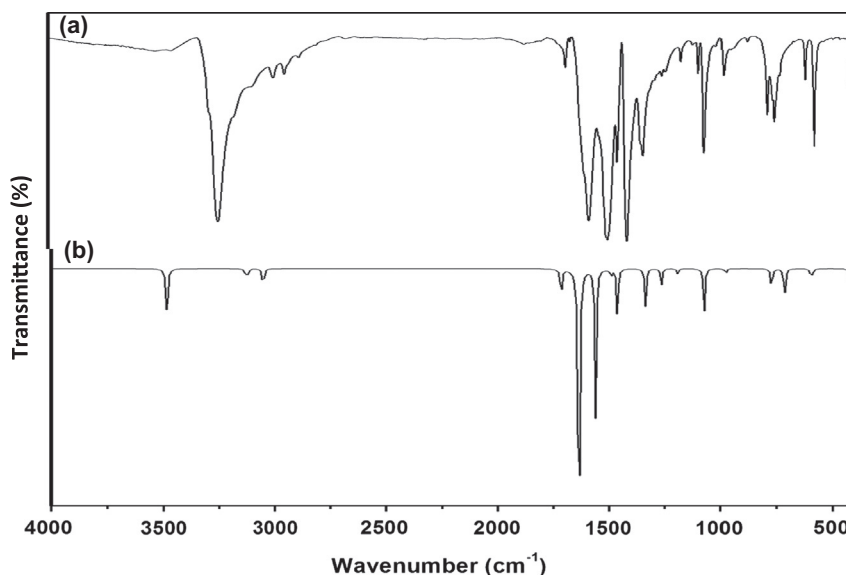
Six normal modes of vibrations $2\nu(\text{N–CH}_3)$, $2\gamma(\text{N–CH}_3)$, $2\alpha(\text{C–N–CH}_3)$ arise due to two (N–CH₃) bonds. Out of the two $\nu(\text{N–CH}_3)$, the i.p. coupled $\nu(\text{N–CH}_3)$ is calculated to have magnitude 978 cm^{-1} (A_g species) and o.p. coupled $\nu(\text{N–CH}_3)$ at frequency 1024 cm^{-1} (B_u species). The magnitude 55 and 116 cm^{-1} correspond to the modes i.p. coupled $\gamma(\text{N–CH}_3)$ (B_g species) and o.p. coupled $\gamma(\text{N–CH}_3)$ (A_u species) respectively. The i.p. coupled angle deformation mode $\alpha(\text{C–N–CH}_3)$ is observed at frequency 267 cm^{-1} (A_g species) and o.p. coupled $\alpha(\text{N–C–CH}_3)$ mode is at 367 cm^{-1} wave number (B_u species).

(C–NHCH₃) modes (6 modes)

There are six normal modes of vibrations arise due to $2(\text{C–NHCH}_3)$ bonds, as $2\nu(\text{C–NHCH}_3)$, $2\beta(\text{C–NHCH}_3)$ and $2\gamma(\text{C–NHCH}_3)$. The frequencies 1208 and 1209 cm^{-1} corresponds to o.p. coupled $\nu(\text{C–NHCH}_3)$ of B_u species and i.p. coupled $\nu(\text{C–NHCH}_3)$ of A_g species respectively. the planar C–NHCH₃ bending mode of i.p. coupled type (A_g species) is found to have magnitude 453 cm^{-1} whereas o.p. coupled C–NHCH₃ planar bending mode appears to have a magnitude 185 cm^{-1} (B_u species). Similarly the non-planar bending mode $\gamma(\text{C–NHCH}_3)$ of i.p. coupled type (B_g species) is calculated to have frequency 128 cm^{-1} and the mode $\gamma(\text{C–NHCH}_3)$ of o.p. coupled type (A_u species) at the frequency 29 cm^{-1} .

N–H modes (6 modes)

The bonds $\text{N}_{11}\text{–H}_{12}$ and $\text{N}_{13}\text{–H}_{14}$ give rise to have 6 normal modes of vibration as $2\nu(\text{N–H})$, $2\beta(\text{N–H})$ and $2\gamma(\text{N–H})$ modes. The wave numbers 3323 cm^{-1} and 3328 cm^{-1} correspond to the i.p. coupled and o.p. coupled (N–H) stretching vibrations respectively. The i.p. coupled $\beta(\text{N–H})$ and o.p. coupled $\beta(\text{N–H})$ modes are calculated to have magnitude 1487 cm^{-1} (A_g species) and 1490 cm^{-1} (B_u species) respectively. The i.p. coupled and o.p. coupled non-planar deformation modes $\gamma(\text{N–H})$ are observed at equal frequency 698 cm^{-1} .

**Fig. 4.** Comparison of observed and calculated infrared spectra of dmb. (a) Observed and (b) calculated spectra.

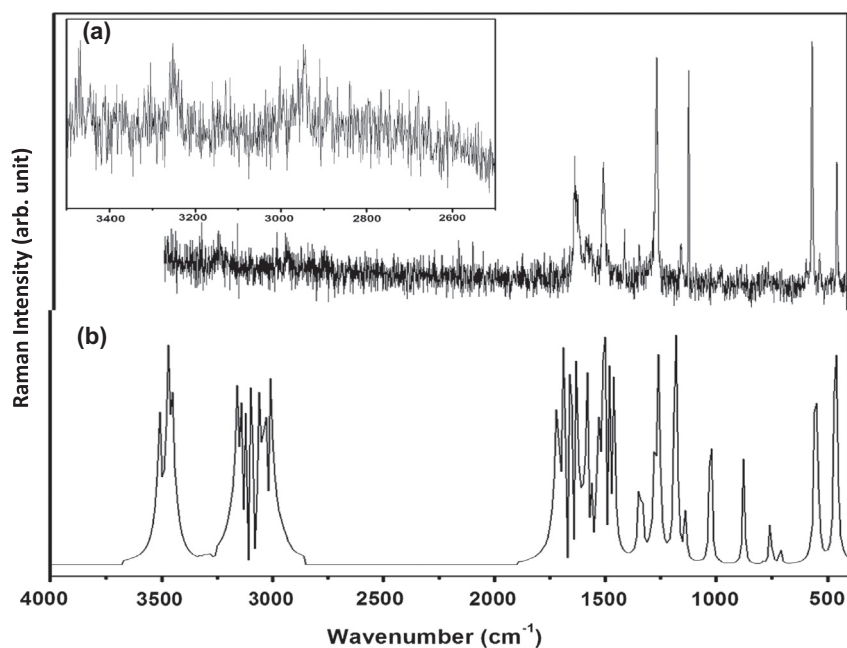


Fig. 5. Comparison of observed and calculated Raman spectra of dmdb. (a) Observed and (b) calculated spectra.

Table 4

Normal modes distribution of dmdb molecule.

S. no.	Modes	Total no.	Symbol	Groups	No. of modes
1	Stretching	22	ν	$C^{15}H_3$, $C^{16}H_3$ C_1-Cl , C_4-Cl $C_2=O$, $C_5=O$ C_3-N , C_6-N $N_{11}-C$, $N_{13}-C$ $N_{11}-H$, $N_{13}-H$ Ring	6 2 2 2 2 2 6
2	Planar deformation ^a	11	β	C_1-Cl , C_4-Cl $C_2=O$, $C_5=O$ C_3-N , C_6-N $N_{11}-H$, $N_{13}-H$ Ring	2 2 2 2 3
3	Non-planar deformation ^a	13	$\alpha(R)$ γ	C_1-Cl , C_4-Cl $C_2=O$, $C_5=O$ C_3-N , C_6-N $N_{11}-H$, $N_{13}-H$ $N_{11}-CH_3$, $N_{13}-CH_3$ Ring	2 2 2 2 2 3
4	Twisting or torsion	2	$\phi(R)$ τ	$C^{15}H_3$ $C^{16}H_3$	1 1
5	Rocking	4	ρ	$\rho_{ }(C^{15}H_3)$ $\rho_{\perp}(C^{15}H_3)$ $\rho_{ }(C^{16}H_3)$ $\rho_{\perp}(C^{16}H_3)$	1 1 1 1
6	Deformation	6	δ	$\delta_s(C^{15}H_3)$ $\delta_{as}(C^{15}H_3)$, $\delta_s(C^{16}H_3)$, $\delta_{as}(C^{16}H_3)$	1 2 1 2
7	Angle Bending	2	α	C_3-N-CH_3 , C_6-N-CH_3	2

^a With respect to the local plane.

NBO analysis

NBO theory allows assignment of the hybridization of atomic lone pairs and of the atoms involved in bond orbital. Interaction

between the atomic orbitals can be interpreted using the NBO which also gives accurate natural Lewis structure of Schrodinger wave function Ψ since it gives the maximum percentage of electron density using mathematical formulation of the orbitals. The

Table 5
Calculated and observed vibrational frequencies and assignments for dmb molecule (C-I).

S. No.	Theoretical wave number		Experimental wave number		(IR, Raman) Depolar-P	Species	Assigned modes	Vibrational assignment (%PED)
	Unscaled	Scaled ^a	IR	Raman				
1	30	29	-	-	(7, 0) 0	A _u	γ(C-NHCH ₃), O.P.C.	τ(C ₆ -N ₁₃) [21], τ(C ₃ -N ₁₁) [21], φ(R) [18], φ(R) [15], γ(N ₁₃ -H ₁₄) [7], γ(N ₁₁ -H ₁₂) [7]
2	56	55	-	-	(0, 1) 0.75	B _g	γ(N-CH ₃), I.P.C.	τ(C ₆ -N ₁₃) [24], τ(C ₃ -N ₁₁) [24], φ(R) [19], γ(N ₁₃ -H ₁₄) [14], γ(N ₁₁ -H ₁₂) [14]
3	66	64	-	-	(2, 0) 0	A _u	φ(R), O.P.C.	φ(R) [46], φ(R) [41]
4	118	116	-	-	(0, 0) 0	A _u	γ(N-CH ₃), O.P.C.	γ(N ₁₃ -H ₁₄) [24], γ(N ₁₁ -H ₁₂) [24], φ(R) [16], τ(C ₆ -N ₁₃) [10], τ(C ₃ -N ₁₁) [10]
5	131	128	-	-	(0, 0) 0.75	B _g	γ(C-NHCH ₃), I.P.C.	φ(R) [32], γ(N ₁₁ -H ₁₂) [17], γ(N ₁₃ -H ₁₄) [17]
6	173	169	-	-	(0, 0) 0	A _u	τ(CH ₃), O.P.C.	τ(C ₆ -N ₁₃) [36], τ(N ₁₁ -C ₁₆) [36]
7	176	172	-	-	(0, 3) 0.75	B _g	τ(CH ₃), I.P.C.	τ(N ₁₁ -C ₁₆) [31], τ(N ₁₃ -C ₁₅) [31], φ(R) [17]
8	189	185	-	-	(3, 0) 0	B _u	β(C-NH-CH ₃), O.P.C.	β(C ₆ -N ₁₃) [21], β(C ₄ -Cl ₉) [21], β(C ₃ -N ₁₁) [12], β(C ₆ -N ₁₃) [12], β(C ₆ -N ₁₃) [11], δ(N ₁₁ -H ₁₂) [11]
9	199	194	-	-	(1, 0) 0	A _u	γ(C-Cl), O.P.C.	γ(C ₄ -Cl ₉)(25), γ(C ₁ -Cl ₁₀)(25), φ(R) [16], τ(C ₃ -N ₁₁) [6], τ(C ₆ -N ₁₃) [6]
10	221	217	-	-	(0, 2) 0.59	A _g	β(C-Cl) + β(C-NCH ₃), I.P.C.	β(C ₁ -Cl ₁₀) [27], β(C ₄ -Cl ₉) [27] β(C ₆ -N ₁₃) [16], β(C ₃ -N ₁₁) [16], α(R)(7)
11	230	225	-	-	(3, 0) 0	B _u	β(C-Cl), O.P.C.	β(C ₄ -Cl ₉) [27], β(C ₁ -Cl ₁₀) [27], β(C ₃ -N ₁₁)(15), β(C ₆ -N ₁₃) [15]
12	273	267	-	-	(0, 12) 0.50	A _g	α(C-N-CH ₃), I.P.C.	β(N ₁₃ -H ₁₄) [22], β(N ₁₁ -H ₁₂) [22], β(C ₁ -Cl ₁₀) [19], β(C ₄ -Cl ₉) [19]
13	280	274	-	-	(0, 6) 0.60	A _g	α(R), I.P.C.	α(R) [28], φ(R) [12], ν(C ₁ -C ₆) [8], ν(C ₅ -C ₆) [8], ν(C ₁ -Cl ₁₀) [7], ν(C ₄ -Cl ₉) [7]
14	281	275	-	-	(0, 1) 0.74	B _g	γ(C-Cl), I.P.C.	γ(C ₁ -Cl ₁₀) [38], γ(C ₄ -Cl ₉) [38], φ(R) [15]
15	348	340	-	-	(0, 10) 0.63	A _g	α(R), I.P.C.	α(R) [35], ν(C ₄ -C ₅) [7], (C ₁ -C ₆) [7]
16	375	367	-	369 vs	(4, 0) 0	B _u	α(C-N-CH ₃), O.P.C.	δ(N ₁₁ -H ₁₂) [18], δ(N ₁₃ -H ₁₄) [18], ν(C ₁ -Cl ₁₀) [13], ν(C ₄ -Cl ₉) [13], β(C ₅ -C ₆) [10]
17	423	414	412 s	426 w	(45, 0) 0	B _u	β(C=O), O.P.C.	β(C ₂ -O ₈) [23], β(C ₅ -O ₇) [23], ν(C ₅ -C ₆) [7], ν(C ₂ -C ₃) [7]
18	463	453	-	472 w	(0, 24) 0.13	A _g	β(C-NHCH ₃), I.P.C.	α(R) [30], α(R) [13], δ(N ₁₁ -H ₁₂) [10], β(N ₁₃ -H ₁₄) [7], ν(C ₂ -C ₃) [7]
19	535	524	-	-	(0, 1) 0.75	B _g	γ(C=O), I.P.C.	γ(C ₃ -N ₁₁) [30], γ(C ₆ -N ₁₃) [30], γ(C ₅ -O ₇) [8], γ(C ₂ -O ₈) [8]
20	553	541	-	-	(0, 21) 0.13	A _g	ν(R) (breathing), I.P.C.	α(R) [13], δ(N ₁₁ -H ₁₂) [9], δ(N ₁₃ -H ₁₄) [9], β(C ₅ -O ₇) [9], β(C ₂ -O ₈) [9], ν(C ₂ -C ₃) [9], ν(C ₁ -Cl ₁₀) [9]
21	589	577	573 s	584 vs	(30, 0) 0	A _u	φ(R), O.P.C.	φ(R) [19], γ(C ₃ -N ₁₁) [17], γ(C ₆ -N ₁₃) [17], γ(C ₁ -Cl ₁₀) [14], γ(C ₄ -Cl ₉) [14]
22	601	588	613s	611w	(14, 0) 0	B _u	α(R) + α(C-N-C), O.P.C.	α(R) [23], δ(N ₁₁ -H ₁₂) [14], β(N ₁₃ -H ₁₄) [14], ν(C ₄ -Cl ₉) [7], ν(C ₁ -Cl ₁₀) [7]
23	714	698	-	-	(0, 1) 0.75	B _g	γ(N-H), I.P.C.	γ(N ₁₁ -H ₁₂) [18], γ(N ₁₃ -H ₁₄) [18], τ(C ₃ -N ₁₁) [17], τ(C ₆ -N ₁₃) [17], φ(R) [8]
24	714	699	-	-	(126, 0) 0	A _u	γ(N-H), O.P.C.	γ(N ₁₃ -H ₁₄) [25], γ(N ₁₁ -H ₁₂) [25], τ(C ₆ -N ₁₃) [20], τ(C ₃ -N ₁₁) [20]
25	757	741	752 s	-	(0, 2) 0.75	B _g	φ(R), I.P.C.	φ(R) [29], γ(C ₅ -O ₇) [19], γ(C ₂ -O ₈) [19], γγ(C ₃ -N ₁₁) [10], γ(C ₆ -N ₁₃) [10]
26	764	748	-	-	(3, 0) 0	A _u	γ(C=O), O.P.C.	γ(C ₂ -O ₈) [29], γ(C ₅ -O ₇) [29], φ(R) [14], γ(C ₃ -N ₁₁) [13], γ(C ₆ -N ₁₃) [13]
27	773	757	-	-	(76, 0) 0	B _u	ν(C-Cl), O.P.C.	α(R) [20], ν(C ₄ -Cl ₉) [20], ν(C ₁ -Cl ₁₀) [20], β(C ₅ -O ₇) [7], β(C ₂ -O ₈) [7]
28	789	773	783 s	-	(0, 0) 0.22	A _g	β(C=O), I.P.C.	β(C ₂ -O ₈) [19], β(C ₅ -O ₇) [19], β(C ₃ -N ₁₁) [13], β(C ₆ -N ₁₃) [13], β(C ₁ -Cl ₁₀) [7], β(C ₄ -Cl ₉) [7]
29	879	860	-	837 w	(0, 5) 0.20	A _g	ν(C-Cl), I.P.C.	ν(C ₄ -Cl ₉) [18], ν(C ₁ -Cl ₁₀) [18], ν(C ₅ -C ₆) [15], ν(C ₂ -C ₃) [15]
30	978	957	977 s	944 w	(17, 0) 0	B _u	ν(R)+ρ(CH ₃), O.P.C.	ν(C ₅ -C ₆) [15], ν(C ₂ -C ₃) [15], β(C ₃ -N ₁₁) [10], β(C ₆ -N ₁₃) [10]
31	1025	978	-	1026 w	(0, 9) 0.38	A _g	ν(N-CH ₃), I.P.C.	ν(N ₁₁ -C ₁₆) [29], ν(N ₁₃ -C ₁₅) [29]
32	1073	1024	1065 vs	-	(156, 0) 0	B _u	ν(N-CH ₃), O.P.C.	ν(N ₁₃ -C ₁₅) [22], ν(N ₁₁ -C ₁₂) [22], α(R) [19], ν(C ₂ -C ₃) [10], ν(C ₅ -C ₆) [10]
33	1138	1087	-	-	(0, 0) 0	A _u	ρ(CH ₃), O.P.C.	δ(C ₁₆ -H ₂₁) [45], β(C ₁₅ -H ₁₇) [34], β(C ₁₅ -H ₁₈) [12]
34	1139	1087	-	-	(0, 2) 0.75	B _g	ρ(CH ₃), I.P.C.	δ(C ₁₆ -H ₂₂) [45], δ(C ₁₅ -H ₁₇) [34], β(C ₁₅ -H ₁₈) [12]
35	1182	1129	1168 s	-	(0, 23) 0.51	A _g	ρ(CH ₃), I.P.C.	δ(C ₁₆ -H ₂₀) [25], β(C ₁₅ -H ₁₇) [18]
36	1191	1138	-	-	(19, 0) 0	B _u	ρ(CH ₃), O.P.C.	δ(C ₁₆ -H ₂₀) [25], β(C ₁₅ -H ₁₇) [21], β(C ₁₅ -H ₁₇) [7]
37	1265	1208	-	1236 w	(60, 0) 0	B _u	ν(C-NHCH ₃), O.P.C.	α(R) [13], β(C ₃ -N ₁₁) [7], β(C ₆ -N ₁₃) [7]
38	1266	1209	-	1284 vs	(0, 43) 0.28	A _g	ν(C-NHCH ₃), I.P.C.	β(C ₅ -C ₆ -C ₁) [12], ν(C ₄ -C ₅) [9], ν(C ₂ -C ₃) [9], ν(C ₆ -N ₁₃) [7], ν(C ₃ -N ₁₁) [7]
39	1337	1277	1338 s	1334 w	(141, 0) 0	B _u	ν(R), O.P.C.	ν(C ₄ -C ₅) [21], ν(C ₁ -C ₆) [21], ν(C ₅ -C ₆) [8], ν(C ₂ -C ₃) [8]
40	1341	1280	1342 sh	1352 w	(0, 13) 0.69	A _g	ν(R), I.P.C.	ν(C ₁ -C ₂) [20], ν(C ₄ -C ₅) [20], ν(C ₆ -N ₁₃) [7], ν(C ₃ -N ₁₁) [7]
41	1463	1397	1409 vs	1409w	(185, 0) 0	B _u	δ _s (CH ₃), O.P.C.	δ(C ₁₅ -H ₁₇) [44], δ(C ₁₆ -H ₂₀) [44]
42	1466	1400	-	1478 w	(0, 17) 0.62	A _g	δ _s (CH ₃), I.P.C.	δ(C ₁₆ -H ₂₀) [45], δ(C ₁₅ -H ₁₇) [45]
43	1490	1423	-	1484w	(25, 0) 0	A _u	δ _{as} (CH ₃), O.P.C.	δ(C ₁₆ -H ₂₁) [34], δ(C ₁₅ -H ₁₈) [34], β(C ₁₅ -H ₁₇) [12], β(C ₁₆ -H ₂₂) [11]
44	1490	1423	1495 vs	1490w	(0, 30) 0.75	B _g	δ _{as} (CH ₃), I.P.C.	δ(C ₁₆ -H ₂₁) [34], δ(C ₁₅ -H ₁₈) [34], β(C ₁₅ -H ₁₇) [12], δ(C ₁₆ -H ₂₂) [11]
45	1508	1440	-	-	(3, 0) 0	B _u	δ _{as} (CH ₃), O.P.C.	β(C ₁₅ -H ₂₂) [31], β(C ₁₅ -H ₁₇) [31], δ(C ₁₅ -H ₁₈) [10], δ(C ₁₆ -H ₂₁) [10]
46	1508	1440	-	-	(0, 6) 0.75	A _g	δ _{as} (CH ₃), I.P.C.	δ(C ₁₆ -H ₂₂) [31], β(C ₁₅ -H ₁₇) [31], δ(C ₁₅ -H ₁₈) [10], δ(C ₁₆ -H ₂₁) [10], δ(C ₁₆ -H ₂₀) [10]

Table 5 (continued)

S. No.	Theoretical wave number		Experimental wave number		(IR, Raman) Depolar-P	Species	Assigned modes	Vibrational assignment (%PED)
	Unscaled	Scaled ^a	IR	Raman				
47	1557	1487	–	–	(0, 159)0.27	A _g	β(N–H), I.P.C.	β(N ₁₃ –H ₁₄) [24], β(N ₁₁ –H ₁₂) [24], ν(C ₃ –C ₄) [8], ν(C ₆ –C ₇) [8]
48	1560	1490	1580	–	(548, 0) 0	B _u	β(N–H), O.P.C.	β(N ₁₁ –H ₁₂) [29], β(N ₁₃ –H ₁₄) [29]
49	1636	1562	–	–	(1351, 0) 0	B _u	ν(R), O.P.C.	ν(C ₃ –C ₄) [22], ν(C ₁ –C ₆) [22], ν(C ₃ –N ₁₁) [11], ν(C ₆ –N ₁₃) [11], ν(C ₅ –O ₇) [7], ν(C ₂ –O ₈) [7]
50	1642	1568	–	–	(0, 47)0.39	A _g	ν(R), I.P.C.	ν(C ₁ –C ₆) [16], ν(C ₃ –C ₄) [16], ν(C ₆ –N ₁₃) [15], ν(C ₃ –N ₁₁) [15], α(R) [9]
51	1693	1617	–	–	(0, 188)0.23	A _g	ν(C=O), I.P.C.	ν(C ₂ –O ₈) [38], ν(C ₅ –O ₇) [38]
52	1715	1638	1684	–	(114, 0) 0	B _u	ν(C=O), O.P.C.	ν(C ₂ –O ₈) [29], ν(C ₅ –O ₇) [29]–α(R) [9], ν(C ₆ –N ₁₃) [7], ν(C ₃ –N ₁₁) [7]
53	3052	2915	2945	–	(75, 0) 0	B _u	ν _s (CH ₃), O.P.C.	ν(C ₁₅ –H ₁₉) [18], ν(C ₁₆ –H ₂₁) [18], ν(C ₁₅ –H ₁₇) [18], ν(C ₁₆ –H ₂₂) [18], ν(C ₁₅ –H ₁₈) [13], ν(C ₁₆ –H ₂₀) [13]
54	3053	2915	2995	–	(0, 541)0.08	A _g	ν _s (CH ₃), I.P.C.	ν(C ₁₆ –H ₂₁) [25], ν(C ₁₅ –H ₁₉) [18], ν(C ₁₆ –H ₂₂) [18], ν(C ₁₅ –H ₁₇) [18], ν(C ₁₆ –H ₂₀) [13], ν(C ₁₅ –H ₁₈) [13]
55	3119	2978	–	2943	(19, 0) 0	A _u	ν _{as} (CH ₃), O.P.C.	ν(C ₁₆ –H ₂₁) [25], ν(C ₁₅ –H ₁₉) [25], ν(C ₁₆ –H ₂₂) [25], ν(C ₁₅ –H ₁₇) [25]
56	3119	2978	–	–	(0, 111)0.75	B _g	ν _{as} (CH ₃), I.P.C.	ν(C ₁₅ –H ₁₉) [25], ν(C ₁₆ –H ₂₁) [25], ν(C ₁₅ –H ₁₇) [25], ν(C ₁₆ –H ₂₂) [25]
57	3131	2990	–	–	(27, 0) 0	B _u	ν _{as} (CH ₃), O.P.C.	ν(C ₁₆ –H ₂₀) [37], ν(C ₁₅ –H ₁₈) [37], ν(C ₁₆ –H ₂₂) [7], ν(C ₁₅ –H ₁₇) [7]
58	3131	2990	3241	–	(0, 168)0.67	A _g	ν _{as} (CH ₃), I.P.C.	ν(C ₁₅ –H ₁₈) [37], ν(C ₁₆ –H ₂₀) [37], ν(C ₁₅ –H ₁₇) [7], ν(C ₁₆ –H ₂₂) [7]
59	3479	3323	–	3255	(0, 254) 0.21	A _g	ν(N–H), I.P.C.	ν(N ₁₁ –H ₁₂) [50], ν(N ₁₃ –H ₁₄) [50]
60	3485	3328	3453	–	(254, 0) 0	B _u	ν(N–H), O.P.C.	ν(N ₁₃ –H ₁₄) [50], ν(N ₁₁ –H ₁₂) [50]

The no. after the modes are the % potential energy calculated using normal coordinate analysis in the last column. The abbreviations are – ν = stretching, τ = twisting, ρ = rocking, γ = out-of-plane deformation, β = in-plane deformation, α(R) = planar ring deformation, φ(R) = non-planar ring deformation, α = angle bending and δ = deformation, s: strong, vs: very strong, m: medium, w: weak, vw: very weak.

^a Calculated wave numbers below 1000 cm⁻¹ were scaled by the scale factor 0.9786 and those above 1000 cm⁻¹ by the scale factor 0.9550 for larger wave numbers.

NBO calculations were performed at the DFT/B3LYP level using NBO 3.1 program incorporated in the Gaussian 09 package.

From Table 6, it is clear that the BD(1)C₂–O₈ orbital having 1.99019 electrons has 36.86% C₂ character in a sp^{2.45} hybrid and 63.14% O₈ character in a sp^{1.50} hybrid. The sp^{2.45} hybrid on C has 70.94% p-character and the sp^{1.50} hybrid on O has 59.91% p-character. The BD(1)C₅–O₇ orbital with 1.98744 electrons has 36.76% C₅ character in a sp^{2.59} hybrid and 63.24% O₇ character in a sp^{1.49} hybrid. The sp^{2.59} hybrid on C has 72.07% p-character, and the sp^{1.49} hybrid on O has 59.81% p-character. An idealized sp³ hybrid has 75% p-character. The coefficients 0.6071, 0.7946, 0.6063 and 0.7953 are called polarization coefficients of dmdb. The role of the two hybrids in the formation of the bond can be determined by the sizes of these coefficients. The oxygen has larger percentage of NBO in both orbitals, which yields the larger polarization coefficient because of its higher electronegativity. Similar results have been found in all the BD(1)C₁–Cl₁₀ and BD(1)C₄–Cl₉ orbitals. The lone pairs which are expected to attain the Lewis structure are given at the end of Table 6.

Molecular electrostatic potential and electrostatic potential

Molecular electrostatic potential (MESP) and electrostatic potential (ESP), useful quantities to illustrate the charge distributions of molecules, are used to visualize variably charged regions of a molecule. Therefore, the charge distributions can give the information about how the molecules interact with another molecule. At any given point $r(x, y, z)$ in the vicinity of a molecule, the molecular electrostatic potential (MEP), $V(r)$ is defined in terms of the interaction energy between the electrical charge generated from the molecule electrons and nuclei and a positive test charge (a proton) located at r [40,41]. The molecular electrostatic potential is related to the electronic density and a very useful descriptor for determining sites for electrophilic attack and nucleophilic reactions as well as hydrogen-bonding interactions [42–44]. In Fig. 6(d), whereas

electrophilic reactivity is presented by the negative (red¹) regions, nucleophilic reactivity is shown by the positive (blue) regions of MEP. As seen from Fig. 6, the red region is localized on the vicinity of oxygen and reflects the most electronegative region (excess negative charge) while the yellow colored lines is localized over the aromatic ring and methyl amine group. On the other hand, the nucleophilic reactivity of the molecules is localized on the hydrogen atoms. In this respect, the compound (dmdb) is found to be useful to both bonds metallicity and interact intermolecularly. Based on these results, it can be ascertained that how the change of the chlorine group affects the molecular properties of the compound. One can see from Fig. 6 that the blue color on methyl amine is found to be the predominant because of the positive charge distribution on the molecule. Moreover, according to the ESP (Fig. 6(a and c)) the most negative ESP is spread over the oxygen and chlorine atoms, indicating the delocalization of electrons over the oxygen and chlorine atoms of the molecule which also reveal extended conjugation of the benzene ring with these groups. Furthermore, the total charge density contour map is given in Fig. 6(b).

HOMO–LUMO analysis

The Highest Occupied Molecular Orbital (HOMO) and the Lowest Unoccupied Molecular Orbital (LUMO) (Fig. 7) are the main orbitals participating dominating in chemical stability. The HOMO represents the ability to donate an electron whereas the LUMO represents the ability to receive an electron. The HOMO and LUMO energies were calculated by DFT at the B3LYP level with the 6-311++G** basis set. The HOMO and LUMO pictures of dmdb are shown in Fig. 7. The energies of the HOMO and the LUMO orbitals of the molecule are $E_{\text{HOMO}} = -0.22403$ a.u. and $E_{\text{LUMO}} = -0.11573$ a.u. respectively with the difference between these two, $\Delta E = 0.1083$ a.u.

¹ For interpretation of color in Fig. 6, the reader is referred to the web version of this article.

Table 6
NBO analysis of dmdb molecule (C-I) based on B3LYP/6-311++G** method.

BOND(A-B)	ED/Energy	ED _A %	ED _B %	NBO	S%	P%
BD(1)C ₁ –C ₂	1.96457	50.48	49.52	0.7105 (sp ^{1.79})	35.76	64.17
				0.7037 (sp ^{1.86})	34.96	64.99
BD(1)C ₁ –C ₆	1.97892	50.90	49.10	0.7135 (sp ^{1.70})	37.02	62.95
				0.7007 (sp ^{1.62})	38.17	61.78
BD(1)C ₁ –Cl ₁₀	1.98700	40.35	59.65	0.6352 (sp ^{2.70})	27.04	72.88
				0.7724 (sp ^{1.94})	34.02	65.94
BD(1)C ₂ –C ₃	1.97437	50.19	49.81	0.7084 (sp ^{1.79})	35.77	64.20
				0.7058 (sp ^{1.63})	37.96	61.98
BD(1)C ₂ –O ₈	1.99019	36.86	63.14	0.6071 (sp ^{2.45})	28.95	70.94
				0.7946 (sp ^{1.50})	39.96	59.91
BD(1)C ₃ –C ₄	1.97893	49.09	50.91	0.7006 (sp ^{1.63})	37.95	62.00
				0.7135 (sp ^{1.70})	37.06	62.90
BD(1)C ₃ –N ₁₁	1.98557	46.54	53.46	0.6822 (sp ^{3.18})	23.90	75.93
				0.7311 (sp ^{4.98})	16.64	82.87
BD(1)C ₄ –C ₅	1.96350	50.87	49.13	0.7133 (sp ^{1.80})	35.73	64.21
				0.7009 (sp ^{1.82})	35.47	64.46
BD(1)C ₄ –Cl ₉	1.98705	40.35	59.65	0.6352 (sp ^{2.69})	27.06	72.86
				0.7723 (sp ^{1.94})	34.02	65.94
BD(1)C ₅ –C ₆	1.97153	49.84	50.16	0.7060 (sp ^{1.79})	35.85	64.10
				0.7082 (sp ^{1.66})	37.63	62.32
BD(1)C ₅ –O ₇	1.98744	36.76	63.24	0.6063 (sp ^{2.59})	27.80	72.07
				0.7953 (sp ^{1.49})	40.06	59.81
BD(1)C ₆ –N ₁₃	1.98487	46.51	53.49	0.6820 (sp ^{3.16})	24.03	75.81
				0.7314 (sp ^{4.97})	16.66	82.86
BD(1)N ₁₁ –H ₁₂	1.99134	71.16	28.84	0.8436 (sp ^{2.25})	30.73	69.22
				0.5370 (sp ^{0.00})	99.93	0.07
BD(1)N ₁₁ –C ₁₆	1.99296	62.56	37.44	0.7909 (sp ^{1.84})	35.16	64.81
				0.6119 (sp ^{3.31})	23.18	76.68
BD(1)N ₁₃ –H ₁₄	1.99125	71.16	28.84	0.8436 (sp ^{2.25})	30.72	69.22
				0.5370 (sp ^{0.00})	99.93	0.07
BD(1)N ₁₃ –C ₁₅	1.99271	62.55	37.45	0.7909 (sp ^{1.84})	35.16	64.81
				0.6119 (sp ^{3.31})	23.17	76.69
BD(1)C ₁₅ –H ₁₇	1.98880	60.37	39.63	0.7770 (sp ^{2.82})	26.17	73.76
				0.6295 (sp ^{0.00})	99.96	0.04
BD(1)C ₁₅ –H ₁₈	1.98878	60.38	39.62	0.7770 (sp ^{2.82})	26.19	73.75
				0.6294 (sp ^{0.00})	99.96	0.04
BD(1)C ₁₅ –H ₁₉	1.98706	59.87	40.13	0.7738 (sp ^{3.06})	24.60	75.34
				0.6335 (sp ^{0.00})	99.96	0.04
BD(1)C ₁₆ –H ₂₀	1.98878	60.37	39.63	0.7770 (sp ^{2.82})	26.18	73.76
				0.6295 (sp ^{0.00})	99.96	0.04
BD(1)C ₁₆ –H ₂₁	1.98879	60.37	39.63	0.7770 (sp ^{2.82})	26.18	73.76
				0.6295 (sp ^{0.00})	99.96	0.04
BD(1)C ₁₆ –H ₂₂	1.98706	59.87	40.13	0.7738 (sp ^{3.06})	24.60	75.34
				0.6335 (sp ^{0.00})	99.96	0.04
BD*(1)C ₁ –C ₂	0.05381	49.52	50.48	0.7037 (sp ^{1.79})	35.76	64.17
				0.7105 (sp ^{1.86})	34.96	64.99
BD*(1)C ₁ –C ₆	0.02965	49.10	50.90	0.7007 (sp ^{1.70})	49.10	62.95
				0.7135 (sp ^{1.62})	38.17	61.78
BD*(1)C ₁ –Cl ₁₀	0.02770	59.65	40.35	0.7724 (sp ^{2.70})	27.04	72.88
				0.6352 (sp ^{1.94})	34.02	65.94
BD*(1)C ₂ –C ₃	0.06052	35.77	64.20	0.7058 (sp ^{1.79})	35.77	64.20
				0.7084 (sp ^{1.63})	37.96	61.98
BD*(1)C ₂ –O ₈	0.01465	63.14	36.86	0.7946 (sp ^{2.45})	28.95	70.94
				0.6071 (sp ^{1.50})	39.96	59.91
BD*(1)C ₃ –C ₄	0.02943	50.91	49.09	0.7135 (sp ^{1.70})	37.95	62.00
				0.7006 (sp ^{1.63})	37.06	62.90
BD*(1)C ₃ –N ₁₁	0.02685	53.46	46.54	0.7311 (sp ^{3.18})	23.90	75.93
				0.6822 (sp ^{4.98})	16.64	82.87
BD*(1)C ₄ –C ₅	0.05450	49.13	50.87	0.7009 (sp ^{1.80})	35.73	64.21
				0.7133 (sp ^{1.82})	35.47	64.46
BD*(1)C ₄ –Cl ₉	0.02776	59.65	40.35	0.7723 (sp ^{2.69})	27.06	72.86
				0.6352 (sp ^{1.94})	34.02	65.94
BD*(1)C ₅ –C ₆	0.06094	50.16	49.84	0.7082 (sp ^{1.79})	35.85	64.10
				0.7060 (sp ^{1.66})	37.63	62.32
BD(1)C ₅ –O ₇	0.01594	63.24	36.76	0.7953 (sp ^{2.59})	27.80	72.07
				0.6063 (sp ^{1.49})	40.06	59.81
BD*(1)C ₆ –N ₁₃	0.02695	53.49	46.51	0.7314 (sp ^{3.16})	24.03	75.81
				0.6820 (sp ^{4.97})	16.66	82.86
BD*(1)N ₁₁ –H ₁₂	0.01167	28.84	71.16	0.5370 (sp ^{2.25})	30.73	69.22
				0.8436 (sp ^{0.00})	99.93	0.07
BD*(1)N ₁₁ –C ₁₆	0.00534	37.44	62.56	0.6119 (sp ^{1.84})	35.16	64.81
				0.7909 (sp ^{3.31})	23.18	76.68
BD*(1)N ₁₃ –H ₁₄	0.01168	28.84	71.16	0.5370 (sp ^{2.25})	30.72	69.22
				0.8436 (sp ^{0.00})	99.93	0.07

Table 6 (continued)

BOND(A-B)	ED/Energy	ED _A %	ED _B %	NBO	S%	P%
BD*(1)N ₁₃ –C ₁₅	0.00535	37.45	62.55	0.6119 (sp ^{1.84})	35.16	64.81
				0.7909 (sp ^{3.31})	23.17	76.69
BD*(1)C ₁₅ –H ₁₇	0.01448	39.63	60.37	0.6295 (sp ^{2.82})	26.17	73.76
				0.7770 (sp ^{0.00})	99.96	0.04
BD*(1)C ₁₅ –H ₁₈	0.01453	39.62	60.38	0.6294 (sp ^{2.82})	26.19	73.75
				0.7770 (sp ^{0.00})	99.96	0.04
BD*(1)C ₁₅ –H ₁₉	0.01667	40.13	59.87	0.6335 (sp ^{3.06})	24.60	75.34
				0.7738 (sp ^{0.00})	99.96	0.04
BD*(1)C ₁₆ –H ₂₀	0.01452	39.63	60.37	0.6295 (sp ^{2.82})	26.18	73.76
				0.7770 (sp ^{0.00})	99.96	0.04
BD*(1)C ₁₆ –H ₂₁	0.01450	39.63	60.37	0.6295 (sp ^{2.82})	26.18	73.76
				0.7770 (sp ^{0.00})	99.96	0.04
BD*(1)C ₁₆ –H ₂₂	0.01668	40.13	59.87	0.6335 (sp ^{3.06})	24.60	75.34
				0.7738 (sp ^{0.00})	99.96	0.04
LP(1)N ₁₁	1.69580			(sp ^{1.00})	0.00	100.00
LP(1)N ₁₃	1.69597			(sp ^{1.00})	0.00	100.00
LP(1)Cl ₉	1.99292			(sp ^{0.21})	82.32	17.67
LP(1)Cl ₁₀	1.99292			(sp ^{0.21})	82.32	17.68
LP(1)O ₇	1.98147			(sp ^{0.67})	59.91	40.07
LP(1)O ₈	1.98119			(sp ^{0.67})	60.02	39.96

Thermodynamic function analysis

On the basis of vibrational analysis at DFT/B3LYP/6-311++G** level, the standard statistical thermodynamic functions: heat capacity (C_p), entropy (S) and enthalpy changes (ΔH) for the title compound were obtained from the theoretical harmonic frequencies and are listed in Table 2 (supplementary material). At room temperature heat capacity, entropy and enthalpy changes are found to be 110.8681 J mol⁻¹ K⁻¹, 205.5233 J mol⁻¹ K⁻¹ and 8.550877 kJ mol⁻¹ respectively. From Table 2 (supplementary material), it can be seen that these thermodynamic functions are increasing with temperature ranging from 100 to 1000 K due to the fact that the molecular vibrational intensities increase with temperature [45].

The correlation equations between heat capacity, entropy, enthalpy changes and temperatures were fitted by quadratic formulas and the corresponding fitting factors (R^2) for these thermodynamic properties are 0.992, 0.991 and 0.999, respectively. The corresponding fitting graphs of these are shown in Fig. 1(a–c) (supplementary material) and the equations are given by,

$$C_p = 18.74602 + 0.33471T - 8.63027T^2 \times 10^{-5} \quad (R^2 = 0.9920)$$

$$S = 75.78923 + 0.47320T - 1.27687T^2 \times 10^{-4} \quad (R^2 = 0.9910)$$

$$\Delta H = -1.12513 + 0.03177T + 2.29242T^2 \times 10^{-6} \quad (R^2 = 0.9990)$$

Reactivity descriptors

Chemical reactivity descriptors of compounds such as hardness, chemical potential, softness, electronegativity and electrophilicity index as well as local reactivity have been defined [46–50]. Pauling introduced the concept of electronegativity as the power of an atom in a compound to attract electrons to it. Softness is a property of compound that measures the extent of chemical reactivity. It is the reciprocal of hardness.

$$S = 1/\eta$$

Using Koopman's theorem for closed-shell compounds, η , μ , χ can be defined as

$$\eta = (I - A)/2$$

$$\mu = -(I + A)/2$$

$$\chi = (I + A)/2$$

Table 7 presents these molecular properties.

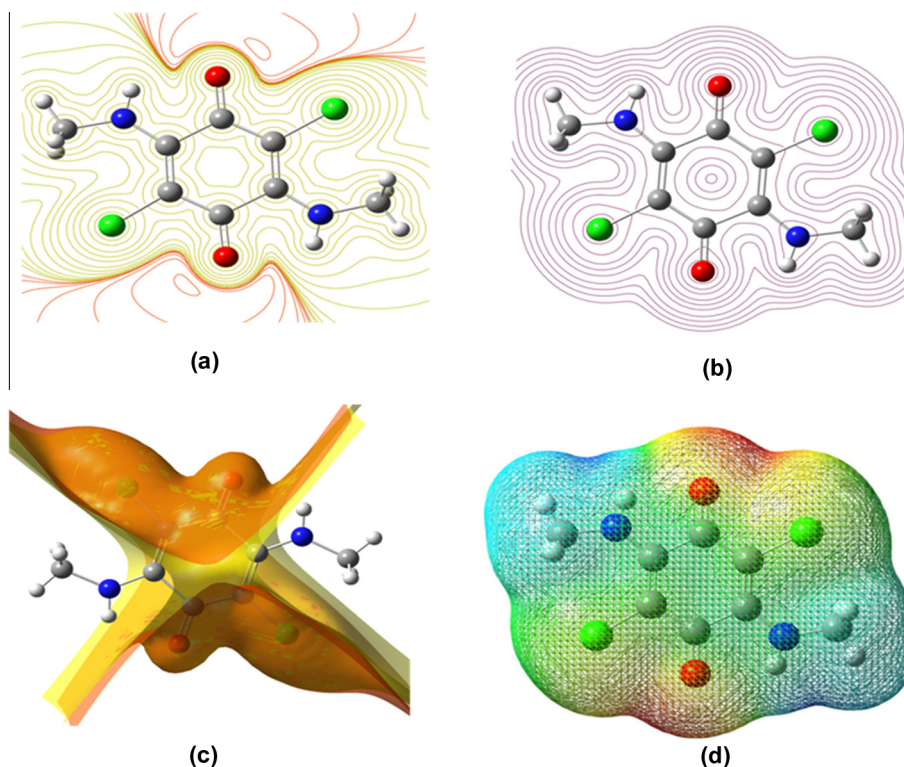


Fig. 6. (a) Contour map, (b) contour map (total density), (c) isosurface plot of ESP and (d) MEP plot of dmdb.

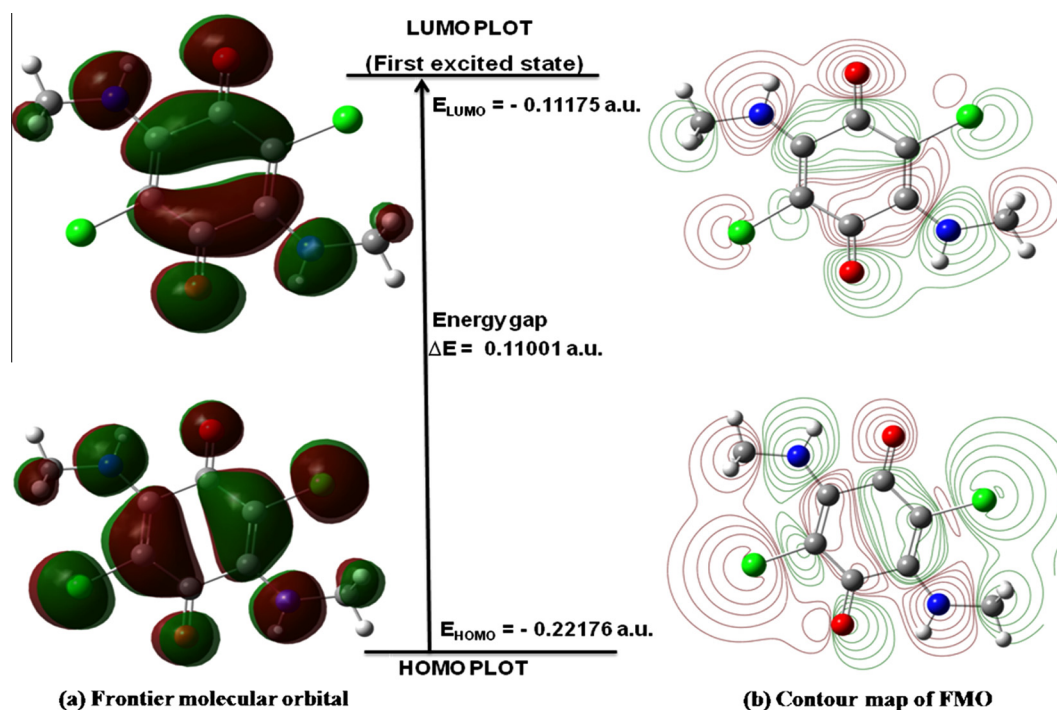


Fig. 7. (a) Frontier molecular orbital and (b) Contour map of FMO of dmdb.

Conclusions

Synthesis and characterization of 2,5-dichloro-3,6-bis-(methylamino)1,4-benzoquinone has been done. FT-IR and FT-Raman spectra of the 2,5-dichloro-3,6-bis-(methylamino)1,4-benzoquinone have been recorded and analyzed. A detailed interpretation

of the observed IR and Raman spectra of 2,5-dichloro-3,6-bis-(methylamino)1,4-benzoquinone is reported on the basis of the calculated potential energy distributions (PEDs). The observed vibrational wave numbers and optimized geometric parameters were seen to be in good agreement with the experimental data. Characteristic vibrational bands of the methylamine and carbonyl

Table 7
Reactivity descriptors and related molecular properties of dmdb.

Molecular properties	Values in eV
Ionization potential (<i>I</i>)	6.0344
Electron affinity (<i>A</i>)	3.0409
Global hardness (<i>η</i>)	1.4968
Electronegativity (<i>χ</i>)	−4.5376
Global softness (<i>s</i>)	0.6681
Chemical potential (<i>μ</i>)	−4.5376
Global electrophilicity (<i>ω</i>)	−13.7564
Band gap	2.9935

groups have been identified. The lowering of HOMO–LUMO energy gap clearly explains the charge transfer interactions taking place within the molecule. The blue color on methyl amine is found to be the predominant because of the positive charge distribution on the molecule according to ESP and the most negative ESP is spread over the oxygen and chlorine atoms, indicating the delocalization of electrons over the oxygen and chlorine atoms of the molecule which also reveal extended conjugation of the benzene ring with these groups. From total charge density contour map it is seen that the red line region is localized over the vicinity of oxygen and chlorine and reflects the most electronegative region (excess negative charge) while the yellow colored lines is localized over the aromatic ring and methyl amine group.

Acknowledgements

Authors are thankful to the Department of Chemistry, Banaras Hindu University, Varanasi for providing the laboratory facilities. Two (BPSG and MS) of the authors are highly grateful to the UGC, New Delhi for the Research fellowships.

Appendix A. Supplementary material

Supplementary data associated with this article can be found, in the online version, at <http://dx.doi.org/10.1016/j.saa.2014.02.082>.

References

- [1] A.R. Amaro, G.G. Oakley, U. Bauer, H.P. Spielmann, L.W. Robertson, *Chem. Res. Toxicol.* 9 (1996) 623.
- [2] P.J. O'Brien, *Chem. Biol. Interact.* 80 (1991) 1.
- [3] R.H. Thomson, *Naturally Occurring Quinones*, vol. 3, Chapman and Hall, London, 1987.
- [4] R.D. Dalton, in: *The Alkaloids*, Academic Press, New York, 1979.
- [5] K. Kaleem, F. Chertok, S. Erhan, *Prog. Organ. Cotings* 15 (1987) 63.
- [6] M. Yoshimoto, H. Miyazawa, H. Nakao, K. Shinkai, M. Arakawa, *J. Med. Chem.* 22 (1979) 491.
- [7] J.S. Driscoll, G.F. Hazard, H.B. Wood, A. Goldin, *Cancer Chemother. Rep. Part 2* 4 (1974) 1.
- [8] A.J. Lin, R.S. Pardini, L.A. Cosby, B.J. Lillis, C.W. Shansky, A.C. Sartorelli, *J. Med. Chem.* 16 (1973) 1268.
- [9] A.J. Lin, B.J. Lillis, A.C. Sartorelli, *Cancer Chemother. Rep. Part 2* 9 (1974) 23.
- [10] C.F. Akl, *Gen. Brit. Patent* 815 (1959) 890.
- [11] P.L. Gutierrez, *Front. Biosci.* 5 (2000) 629.
- [12] R.A. Morton, *Biochemistry of Quinones*, Academic Press, New York, 1965.
- [13] S.P. Gupta, *Chem. Rev.* 94 (1994) 1507.
- [14] P. Schudel, H. Mayer, O. Isler, W.H. Seibrell, R.S. Harris (Eds.), *The Vitamins*, vol. 5, Academic Press, New York, 1972.
- [15] F. Arcamone, *Doxorubicins, Anticancer, Antibiotics*, Academic Press, New York, 1981.
- [16] R. Cassis, M. Scholz, R. Tapia, J.A. Valderrama, *Tetrahedron Lett.* 26 (1985) 6281.
- [17] B.H. Lipshutz, P. Mollard, S.S. Pfeiffer, W. Chrisman, *J. Am. Chem. Soc.* 124 (2002) 14282.
- [18] B.F. Sels, D.E. De Vos, P.A. Jacobs, *Angew. Chem. Int. Ed.* 44 (2005) 310.
- [19] Y. Naruta, K. Maruyama, Recent advances in the synthesis of quinonoid compounds, in: S. Patai, Z. Rappoport (Eds.), *The Chemistry of the Quinonoid Compounds*, vol. 2, Wiley, Chichester, U K, 1998, Part 1.
- [20] P.J. Dudfield, B.M. Trost, I. Fleming (Eds.), *Comprehensive Organic Synthesis*, vol. 7, Pergamon, Oxford, 1991.
- [21] K.T. Finley, *Quinones as synthones*, in: S. Patai, Z. Rappoport (Eds.), *The Chemistry of the Quinonoid Compounds*, vol. 2, Wiley, Chichester, UK, 1988.
- [22] S. Quideau, L. Pouysegou, *Org. Proced. Int.* 31 (1999) 617.
- [23] S. Yamada, T. Takeshita, J. Tanaka, *J. Synth. Org. Chem. Jpn.* 40 (1982) 268.
- [24] S. Patai, *The Chemistry of the Quinoid Compounds*, Wiley, Chichester, 1974.
- [25] B.L. Trumpower, *Functions of Quinones in Energy Converting Systems*, Academic Press, New York, 1982.
- [26] J.P. Klinman, M. David, *Annu. Rev. Biochem.* 63 (1994) 299.
- [27] R.H. Thomson, S. Patai, Z. Rappoport (Eds.), *The Chemistry of the Quinonoid Compounds*, John Wiley & Sons, Bristol, 1974.
- [28] Y. Naruta, K. Maruyama, S. Patai, Z. Rappoport (Eds.), *The Chemistry of the Quinonoid Compounds*, vol. 2, John Wiley & Sons, New York, 1988.
- [29] M. Tisler, *Heterocyclic quinones*, in: A.R. Katritzky (Ed.), *Advances in Heterocyclic Chemistry*, vol. 45, Academic Press, London, 1989, p. 37.
- [30] M.J. Frisch, G.W. Trucks, H.B. Schlegel, G.E. Scuseria, M.A. Robb, J.R. Cheeseman, G. Scalmani, V. Barone, B. Mennucci, G.A. Petersson, H. Nakatsuji, M. Caricato, X. Li, H.P. Hratchian, A.F. Izmaylov, J. Bloino, G. Zheng, J.L. Sonnenberg, M. Hada, M. Ehara, K. Toyota, R. Fukuda, J. Hasegawa, M. Ishida, T. Nakajima, Y. Honda, O. Kitao, H. Nakai, T. Vreven, J.A. Montgomery Jr., J.E. Peralta, F. Ogliaro, M. Bearpark, J.J. Heyd, E. Brothers, K.N. Kudin, V.N. Staroverov, R. Kobayashi, J. Normand, K. Raghavachari, A. Rendell, J.C. Burant, S.S. Iyengar, J. Tomasi, M. Cossi, N. Rega, J.M. Millam, M. Klene, J.E. Knox, J.B. Cross, V. Bakken, C. Adamo, J. Jaramillo, R. Gomperts, R.E. Stratmann, O. Yazyev, A.J. Austin, R. Cammi, C. Pomelli, J.W. Ochterski, R.L. Martin, K. Morokuma, V.G. Zakrzewski, G.A. Voth, P. Salvador, J.J. Dannenberg, S. Dapprich, A.D. Daniels, O. Farkas, J.B. Foresman, J.V. Ortiz, J. Cioslowski, D.J. Fox, *Gaussian 09, Revision A.02*, Gaussian Inc, Wallingford, CT, 2009.
- [31] R. Dennington II, T. Keith, J. Millam, *GaussView, Version 4.1.2*, Semichem Inc., Shawnee Mission, KS, 2007.
- [32] A.D. Becke, *J. Chem. Phys.* 98 (1993) 5648.
- [33] P.J. Stephens, F.J. Devlin, C.F. Chabalowski, M.J. Frisch, *J. Phys. Chem.* 98 (1994) 11623.
- [34] C. Lee, W. Yang, R.G. Parr, *Phys. Rev. B* 37 (1988) 785.
- [35] A. Saiardi, H. Erdjument-Bromage, A.M. Snowman, P. Tempst, S.H. Snyder, *Curr. Biol.* 9 (1999) 1323.
- [36] M.J. Schell, A.J. Letcher, C.A. Brearley, J. Biber, H. Murer, R.F. Irvine, *FEBS Lett.* 461 (1999) 169.
- [37] G. Rauhut, P. Pulay, *J. Phys. Chem.* 99 (1995) 3093–3100.
- [38] R.L. Prasad, A. Kushwaha, Suchita, M. Kumar, R.A. Yadav, *Spectrochimica Acta Part A* 69 (2008) 304.
- [39] R.A. Yadav, R. Shankar, I.S. Singh, *Indian J. Pure Appl. Phys.* 23 (1985) 343.
- [40] N. Ozdemir, B. Eren, M. Dincer, Y. Bekdemir, *Mol. Phys.* 108 (2010) 13.
- [41] P. Politzer, J.S. Murray, *Theor. Chem. Acc.* 108 (2002) 134.
- [42] F.J. Luque, J.M. Lopez, M. Orozco, *Theor. Chem. Acc.* 103 (2000) 343.
- [43] N. Okulik, A.H. Jubert, *Internet electron, J. Mol. Des.* 4 (2005) 17.
- [44] C. Parlak, M. Akdogan, G. Yildirim, N. Karagoz, E. Budak, C. Terzioglu, *Spectrochim. Acta A* 79 (2011) 263.
- [45] J.B. Ott, J. Boerio-Goates, *Calculations from Statistical Thermodynamics*, Academic Press, 2000.
- [46] R.G. Parr, L.V. Szentpaly, S.J. Liu, *J. Am. Chem. Soc.* 121 (1999) 1922.
- [47] P.K. Chattaraj, B. Maiti, U. Sarkar, *J. Phys. Chem. A* 107 (2003) 4973.
- [48] R.G. Parr, R.A. Donnelly, M. Ley, W.E. Palke, *J. Am. Chem. Soc.* 68 (1978) 3807.
- [49] R.G. Parr, R.G. Pearson, *J. Am. Chem. Soc.* 105 (1983) 751.
- [50] R.G. Parr, P.K. Chattaraj, *J. Am. Chem. Soc.* 113 (1991) 1854.